Thermophysics and Aeromechanics, 2007, Vol. 14, No. 3

NONLINEAR INSTABILITY RESEARCH OF LONGITUDINAL STRUCTURE GENERATED BY ROUGHNESS IN UNSWEPT WING BOUNDARY LAYER*

V.G. CHERNORAI, Yu.A. LITVINENKO, V.V. KOZLOV, and G.R. GREK

Khristianovich Institute of Theoretical and Applied Mechanics SB RAS, Novosibirsk, Russia

(*Received February 2, 2007*)

The results of experimental study of a nonlinear varicose instability of the streaky structure generated by roughness element in unswept-wing boundary layer are presented. Features of the varicose breakdown of longitudinal steady streaky structure such as modulation of structure in transverse and streamwise directions by secondary disturbance, occurrence of the new streaky structures and Λ-structures downstream are shown. Spatio-temporal pictures of the hot-wire visualization of flow during spatial evolution of the streaky structures under influence of secondary high-frequency disturbance are discussed. Features of the adverse pressure gradient influence upon processes of the nonlinear varicose instability evolution and flow structure are revealed. Essential influence of the adverse pressure gradient on evolution of disturbances is shown. Comparison of varicose instability of the streaky structures generated in two different ways (the roughness element as in the given work, and continuous air blowing as in the earlier published work) is the carried out.

1. INTRODUCTION

It is known [1] that boundary-layer transition in low-turbulent flow is initiated by wavy disturbances, so-called Tollmien — Schlichting waves. During streamwise evolution they start to grow as small-amplitude perturbations, then turn into nonlinear ones and finally result in flow turbulisation. The linear stage of instability waves development is well understood through theoretical and experimental studies while nonlinear effects, especially close to final laminar flow breakdown, are not so obvious. Generally, in the nonlinear region of laminar-turbulent transition the Tollmien — Schlichting waves undergo three-dimensional deformations resulting in so-called Λ-structures [2–4]. To features of occurrence and development of these structures it is significant that they are typical not only of classical laminar-turbulent transition [2], but also are observed at transition in more complex flows. For example, such structures were revealed in the flows modulated by longitudinal streaky structures at high free stream turbulence [5], in a viscous sublayer of a turbulent boundary layer [6], and also in the flows modulated by Goertler vortices [7–9] or crossflow vortices on swept wings [5], etc. In the given situations they arise, in particular, because of secondary high-frequency instability of such flows and can be shown not only as Λ-structures, but also as Ω-structures, hairpin

* The work was supported by the Ministry of Education and Science of the Russian Federation (Grant No. RNP. 2.1.2.3370) and by the Russian Foundation for Basic Research (Grant No. 05-01-00034).

vortices, etc. vortices. Nevertheless, their general feature is presence of paired counter-rotating longitudinal vortices, so-called "legs" of the Λ-structures, with a "head" in front of them. Just dynamics of these nonlinear structures is responsible for onset of turbulent motion in a number of situations. However, the vortices can be strongly deformed, e.g., in a swept-wing boundary layer where one of the "legs" is suppressed by the crossflow component [5, 10]. The origin and development of the 3D nonlinear perturbations were explored experimentally [5, 10–13] and numerically [14–16]. In these works it was found that the mechanism of turbulence production in various transitional (for example, harmonious and subharmonic types of classical transition) and turbulent near-wall layers is actually one and the same being related to appearance, evolution, and breakdown of the Λ-, Ω-structures, etc.

On the other hand, as was mentioned above, the initial instability of many flows is related to their transverse modulation by steady (Goertler vortices, crossflow vortices on swept wings, etc.) and unsteady (boundary-layer streaks at high free-stream turbulence, Λ-, Ω-, and hairpin vortices, etc.) streamwise vortices. This generates conditions, that is unstable inflectional profiles of velocity normal to the surface $\partial U/\partial y$ and across the flow $\partial U/\partial z$, for origination and growth of secondary high-frequency oscillations whose downstream evolution leads to boundary-layer turbulisation. The streaky structures also have been found in the viscous sublayer of turbulent boundary layer, their contribution to generation of turbulent fluctuations is explored experimentally, analytically, and numerically. The results of direct numerical simulation of turbulent flow in a channel [16] clearly demonstrate formation of perturbations similar to the Λ-structures. Different types of coherent structures occurring in the viscous sublayer of turbulent flow are distinguished in [17].

An important issue is involvement of the coherent structures in turbulisation of jet flows. It was shown in [18, 19] that in circular and plane jets the streaky structures appear directly at the nozzle exit. Then, at their interaction with 2D Kelvin — Helmholtz vortex rings the latter are distorted with formation of azimuthal spikes similar to Λ- or Ω-shaped structures. The scenario of this process resembles the three-dimensional distortion of 2D Tollmien — Schlichting waves at the nonlinear stage of their development. Further, secondary high-frequency disturbances generated in the region of streaky structures origination [18] destroy the azimuthal spikes intensifying mixing of the jet with the ambient fluid and its turbulisation. The high-frequency disturbances evolve on two counter-rotating vortices which are constituents of the Λ- or Ω-shaped azimuthal spikes whose instability to such perturbations was demonstrated in [13]. Thus, the streaky structures dominate not only in near-wall transitional and turbulent flows but also in free shear layers such as circular and plane jets. Mechanisms of their origination, development, and interaction with other disturbances, as well as contribution to the processes of turbulization and regeneration of turbulence are focused on by many researchers.

The high-frequency secondary instabilities of transitional and turbulent flows modulated by the streaky structures are often associated with the so-called sinusoidal and varicose instabilities. For example, flow visualization in case of Goertler vortices [5–7] indicated that the transition process is dominated by secondary mechanisms which produce traveling waves independent of each vortex pair so that the neighboring pairs can amplify different types of secondary motion: either in the form of periodic "meandering" of the vortices in the transverse direction or in the form of horse-shoe bunches in the region of strong transverse shear. Such disturbances are called the sinusoidal and the varicose mode, respectively, being correlated with the odd and even modes known from analytical and numerical results on secondary instability of the Goertler vortices. The secondary perturbations amplify due to the inviscid local mechanism caused by inflections in instantaneous velocity profiles both in the normal (varicose mode) and in the

transverse (sinusoidal mode) directions. Then, the choice of the instability mode excited first and growing most rapidly depends on initial conditions, in particular, on distance between the streamwise perturbations. For example, it was found numerically [20, 21] that the varicose mode is typical of the long-wave vortices, whereas the sinusoidal instability prevails in the short-wave disturbances. The reason is that in the first case a weak transverse shear is induced while in the second one it becomes larger.

Direct numerical simulation of the varicose instability in turbulent boundary layer [22] revealed similarity of the horse-shoe vortices generated in laminar and turbulent boundary layers. Also it was found that the mechanism of horse-shoe vortices generation in turbulent flows is related to an inflectional ($\partial U/\partial y$) instability of the streaky structures. The horse-shoe vortices can induce new streaky structures in the viscous sublayer of turbulent boundary layer that is in agreement with the results of [17]. On the other hand, the sinusoidal instability associated with the transverse inflectional velocity profile ($\partial U/\partial z$) has been confirmed in a series of studies [23–25]. One expects that both types of instability are involved in self-sustaining of turbulence in boundary layers: the sinusoidal one is responsible for regeneration of near-wall turbulence [26–28], and the varicose instability produces the horse-shoe vortices farther from the wall [11, 12, 17, 22, 29].

The both instability modes were examined under controlled conditions at their linear and weakly nonlinear evolution in [30]. When the transverse scale of the streaky structure was larger than the shear-layer thickness, the varicose instability was amplified, otherwise, the structure became more unstable to antisymmetric disturbances than to symmetric ones. The experiments [30] clearly demonstrated that growth of the symmetric mode results in formation of hairpin or Λ-vortices, whereas the antisymmetric mode evolves into a wave train of quasi-streamwise vortices with vorticity of alternating sign. At the same time, experiments at late stages of the nonlinear sinusoidal and varicose instabilities on a flat plate [31] indicated that, finally, in both cases the Λ-vortices are produced with their further multiplication. We notice also the wind-tunnel results [32] on the varicose instability of a solitary streaky structure in swept wing flow revealing that the Λ-vortices become asymmetric due to the crossflow velocity component.

Results of the experimental studies of varicose instability of the streaky structure generated by continuous air blowing in unswept wing boundary layer are presented in work [33]. The nonlinear stage of process in areas with zero and adverse pressure gradients was investigated. It is shown that the adverse pressure gradient results in transverse multiplication of both coherent Λ-vortices and streaky structures and also accelerates flow turbulisation. As against studies of work [33] where the streaky structure has been generated with help of air blowing through a small aperture on a wing surface in this case the streaky structure was generated with the help of a roughness element, as well as in work [30]. Except for the generator of stationary disturbance, other conditions of the given experiment remained same, as well as in work [33]. It was interesting to compare, whether there are features of the streaky structures varicose breakdown depending on a way of its generation, i.e. entry conditions. If in the previous work [33] initial intensity of the stationary disturbance could be adjusted (air blowing) at constant free stream velocity in given situation (roughness) one is connected only to change of a free stream velocity with other things being equal. The basic attention has been devoted on the coherent structures arising during secondary high-frequency varicose instability of the streaky structures, and pressure gradient influence on their development that is important both for understanding of the transition mechanisms to turbulence and for mechanisms of the turbulence regeneration in a turbulent boundary layer for gradient flows.

The time-averaged streamwise component of flow velocity U and its fluctuations u' were measured in space (xyz) and time (t) with help of hot-wire anemometer. This has enabled us to present results of measurements in the form of spatio-temporal hot-wire

visualization pictures of flow and, thus, to reveal features of dynamics of the occurrence, evolution, and internal structure of coherent formations up to later stages of their nonlinear development.

Thus, the purpose of the given work will consist in research of influence of an adverse pressure gradient on the nonlinear varicose instability of the streaky structure generated by roughness element in unswept wing boundary layer and comparison of the obtained results with results of the work [33].

2. EXPERIMENTAL ARRANGEMENT AND PROCEDURE MEASUREMENTS

The experiments were performed in a subsonic low-turbulent wind tunnel with a degree of turbulence $u'/U_0 = 0.04$ % (Fig. 1). In the test section of the facility, a wing model (*1*) with 500-mm chord (*b*) and 1000-mm span was mounted. Due to particular airfoil used in the study streamwise pressure gradient was negligible at the test surface of the wing in the range $x/c \approx 0.22$ to $x/c = 1.0$ from its leading edge at a small negative angle of attack turning the adverse one as incidence increased. A stationary longitudinal structure (further streaky structure) was generated with the help of a roughness element in length of 5.5 mm and height of 0.9 mm located at distance 124 mm from the wing leading edge (see Fig. 1). High-frequency secondary disturbances of the streaky structure were excited at the frequency $f = 333$ Hz by a dynamic loudspeaker connected by a pneumatic line with the two apertures of 1 mm diameter and distance between them of 2.5 mm located on a wing surface at distance 136 mm from the wing leading edge (see Fig. 1). It is to be noted that two apertures intended for generation of a sinusoidal mode secondary instability, but in this case they are used for generating only varicose mode. Axes of coordinates: x — downstream from the wing leading edge, y — on a normal to

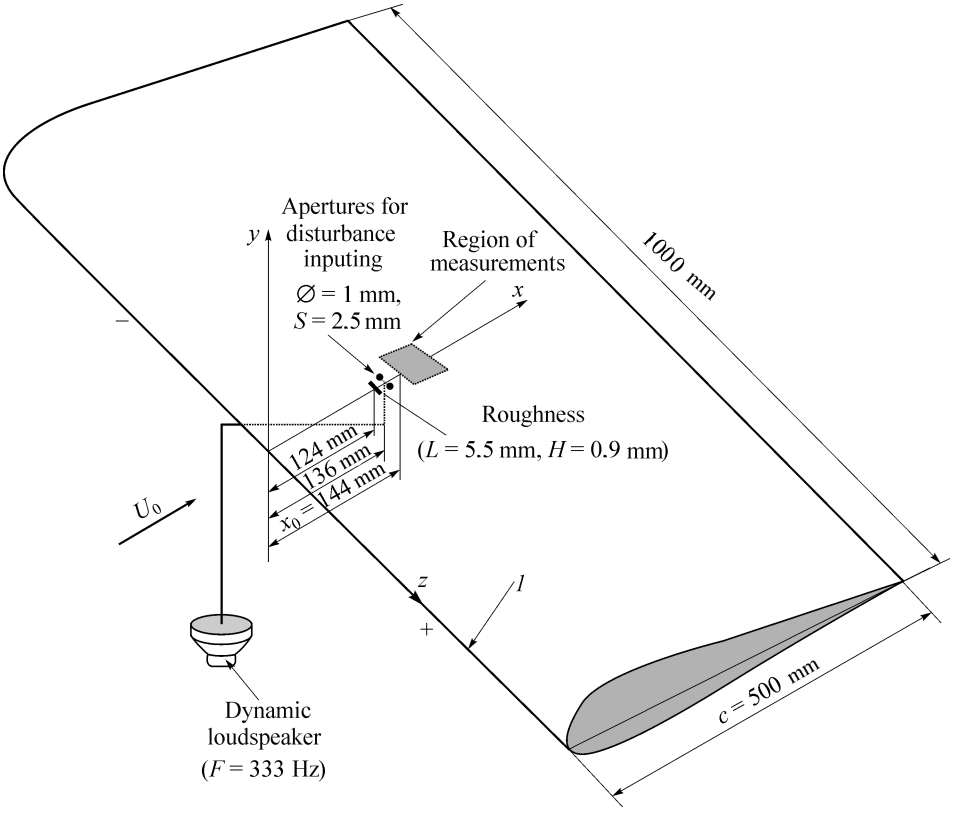

Fig. 1. Experimental model.

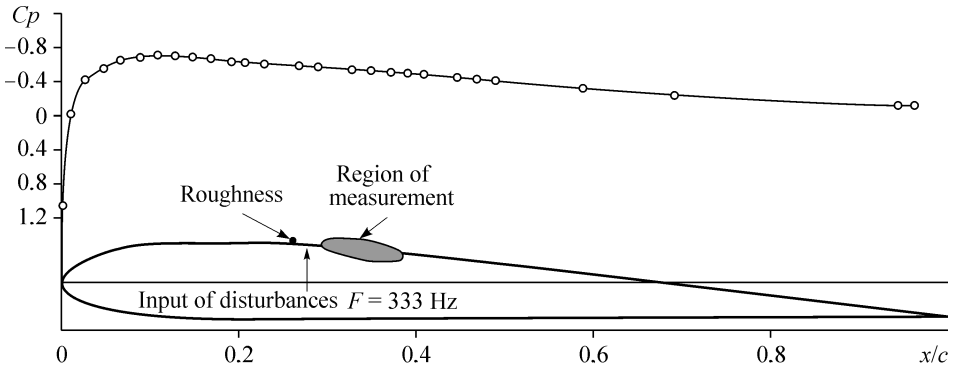

Fig. 2. Pressure curve at the test surface of the wing for the case $dp/dx > 0$.

a surface, and z — transverse direction. The position started areas of measurements x = 144 mm is marked as x_0. Coordinates (x, z) are referred to a chord of model with c = 500 mm. Speed of an accumulating stream made U_0 = 5.5 m/s, the level of turbulence did not exceed 0.04 % of U_0 at U_0 from 5 to 15 m/s in a frequency range from 0.1 up to 10000 Hz.

As against work [33], the case of flow with an adverse gradient of pressure ($dp/dx > 0$) was investigated only. The model was located under a zero angle of attack as in [33], which has provided $dp/dx > 0$ in the region of measurements (Fig. 2). In the absence of artificial disturbances the laminar boundary layer developed without any waves and mean velocity profiles were self-similar in the region of measurements in dimensionless coordinates ($y \to y/\delta^{**}$, where δ^{**} is momentum loss thickness and $U \to U/U_{\max}$) also were close to Blasius profile on a flat plate for a case $dp/dx = 0$ [33]. For the case of an adverse pressure gradient ($dp/dx > 0$) the self-similarity of the mean velocity profiles also may be observed in region of measurements, and their shape corresponded to pre-separated profile with the Hartree parameter m = –0.08 (Fig. 3). It is known [34] that Hartree parameter $m = 0$ corresponds to boundary layer flow with Blasius velocity profile ($dp/dx = 0$), $m > 0$ corresponds to the accelerated flow ($dp/dx < 0$), and $0.0904 < m < 0$ corresponds to the slowed down flow ($dp/dx > 0$). The bottom border of existence of the boundary layer flow without separation corresponds to the Hartree parameter m = –0904. Thus, in this case (m =0.08) development of disturbances will be investigated in the region of still pre-separated flow. The Reynolds number in the measurements region $R^* = \delta^* U_\infty/\nu$, where δ^* is displacement thickness, was within 950 to 1100 at free-stream velocity U_0 = 5.5 m/s. At generation of the streaky structure the velocity profiles became inflexional ones both normally to the wall (y) and in the transverse direction (z). The boundary layer with streaky structure remained laminar in measured areas ($x - x_0 \tilde{=} 0 \to 50$ mm) without excitation of secondary high-frequency disturbances. It has allowed us to control instability by the streaky structures with the help of artificial disturbances introduction through two apertures 1 mm in diameter for excitation of transverse symmetric disturbances (see Fig. 1). Symmetric disturbances were excited by sinusoidal electric signals from oscillator connected with the dynamic loudspeaker. Then, the flow perturbed by the stationary disturbance was subjected to the high-frequency secondary oscillations symmetric in the transverse direction. The excitation frequency f = 333 Hz corresponded to the normalized value $2\pi f\nu/U_0^2 \cdot 10^6 \approx 1037$. The amplitude of secondary disturbances was 7 per cent of U_0 near to a source ($x - x_0$ = = 0 mm), which allowed us to investigate the nonlinear stage of process, which was of basic interest for us.

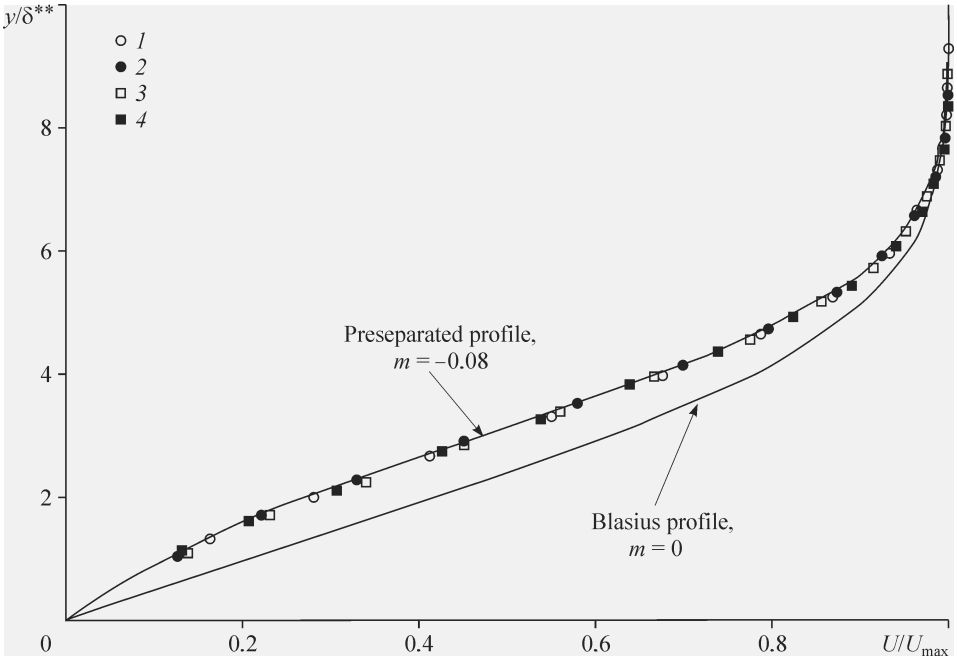

Fig. 3. Boundary layer profiles for the case $dp/dx > 0$.

The hot-wire anemometer measured the time-averaged streamwise component of flow velocity U and its fluctuations u'. The hot-wire probe with gilded tungsten wire 1 mm long and 5 μm in diameter was calibrated in the free stream using the modified King law $U = k_1(E^2 - E_0^2)^{1/n} + k_2(E - E_0)^{1/2}$, where E_0 is output voltage of the anemometer at zero flow velocity, k_1, k_2, and n are adjustable constants with n normally close to 0.5 and k_2 accounting for free convection close to the wall at low flow velocities. The maximum error in probe calibration was within 1 per cent of U_0. All measurements were performed in automatic mode with a traverse system driving the hot-wire probe due to a specially designed program involving LabVIEW. At each point ensemble-averaged traces of the hot-wire signal (up to 50 samples) were recorded with further processing of the data in MatLab environment. In this way, contours of flow velocity in $y - z$ planes as well as spatio-temporal flow patterns of the laminar flow breakdown were investigated.

3. NONLINEAR VARICOSE INSTABILITY IN ADVERSE PRESSURE GRADIENT FLOW

Now we shall consider the flow structure at a nonlinear stage of the streaky structure varicose instability in the unswept wing boundary layer for case of adverse pressure gradient ($dp/dx > 0$) in more detail. In the case $dp/dx > 0$ the effect of secondary nonlinear disturbances on the mean flow is much more pronounced than that at zero pressure gradient [33]. Contours of the mean velocity deviation (ΔU) in yz-plane given in Fig. 4 indicate much stronger spanwise spreading of the perturbed flow area from 5 to 10 mm over the x-range of measurements. Initially ($x/c = 0.289$) the disturbed area consisted of negative mean flow deviations with peak amplitude of 20 % U_0 on an axis and two weak mean flow deviations on both sides from the first with peak amplitude about 8 % U_0 (see Fig. 4). The total amplitude of the mean velocity distortion in the given position is 28 % of U_0. Further downstream, the integrated amplitude of the mean velocity distortion in the beginning reduced to 20 % of U_0, and then increased to 40 % of U_0 at $x/c = 0.379$ in comparison with its magnitude of 28 % of U_0 at $x/c = 0.289$. Structure of the disturbed

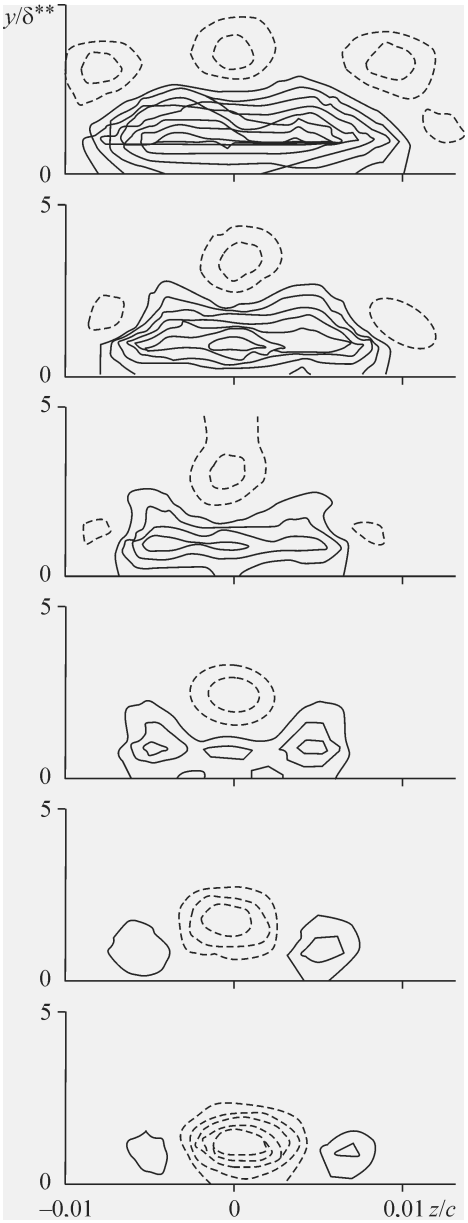

Fig. 4. $y - z$ slices of the mean flow distortion by the streaky structure for x/c positions of 0.289, 0.307, 0.325, 0.343, 0.361, 0.379 (see upwards). Solid and dashed lines indicate positive and negative U-deviations, the contours step is 4 per cent of U_0, y^{**} is momentum thickness.

area downstream was changed as well. The area of positive mean flow defect became prevailing on an axis and near to the wall while the area of negative mean flow defect was split into several small regions located near upper border of the boundary layer. As is obvious from the foregoing this is due to the effect of adverse pressure gradient both on the induced streaky structure and its secondary perturbations.

Now we will consider the secondary high-frequency disturbances evolution. R.m.s. in yz-plane contours given in Fig. 5 illustrate the high rate of the transverse spreading of the secondary oscillations downstream from 5 to 20 mm with their total amplitude growth from 6 to 12 per cent over the testing area. On the other hand, the initially simple structure of the disturbance splits into several closed small areas symmetric by $z/c = 0$. Especially evidently development of secondary disturbances is possible to observe from the 3D flow pattern given in Fig. 6, where isosurfaces of the velocity fluctuation amplitudes ($u' = 1.5$ % of U_0) in (xyz) space are shown. At the initial stage of the disturbances evolution, one can observe a pair of quasi-streamwise vortices which convert downstream into multiplying hairpin and Λ-structures. These vortices are distinctly observed at $x/c \approx 0.34$ and further downstream as alternating positive and negative structures on each period of secondary disturbance. It is possible to observe their transverse multiplication downstream. A similar picture of the secondary disturbance evolution is observed on contours of the velocity fluctuation amplitudes (u') in xz-plane at $y = 1.6$ mm during various moments of time (Fig. 7). One can see the Λ-structures formation process due to the streaky structure modulation by varicose mode of instability according to time sequence of the spatial pictures. It is distinctly observed the transverse spreading of disturbed area.

Figure 8 presents spatial pictures of the secondary high-frequency disturbances evolution together with its influence on average flow characteristics ($u' + \Delta U$) represented in the form of the disturbance amplitude isosurfaces ($u' + \Delta U = 2.5$ % of U_0) for various moments of time, as well as for Fig. 7. It is possible to note occurrence of the new streaky structures arising on both sides from the basic structure in transverse

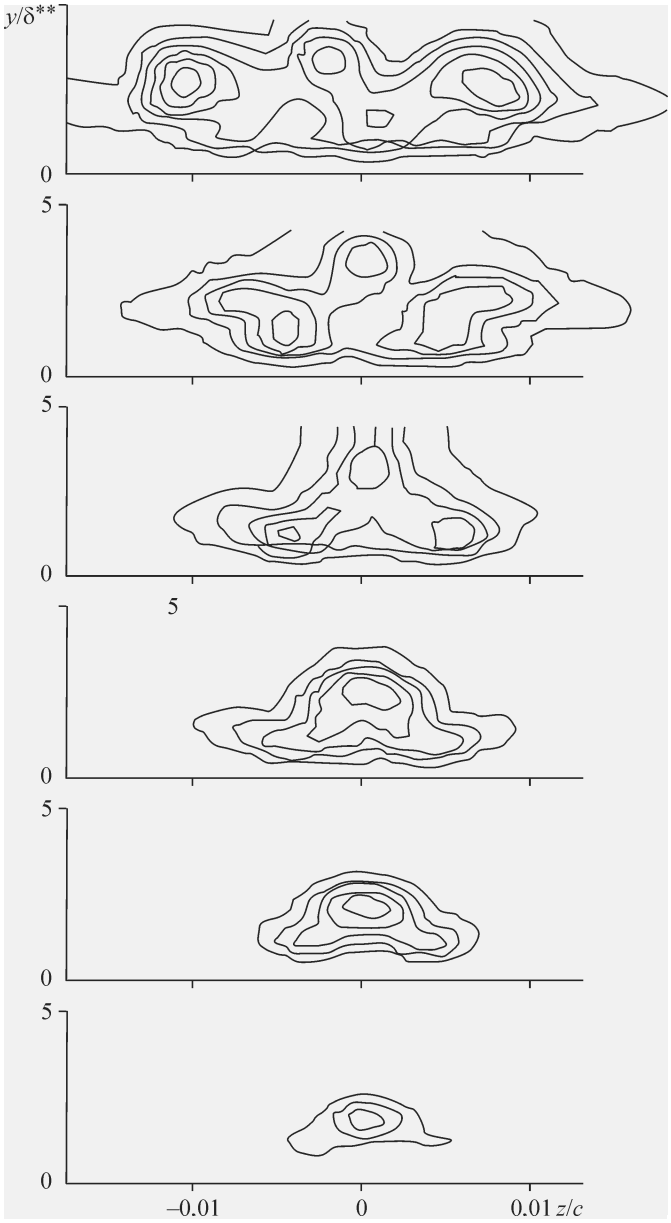

Fig. 5. $y - z$ slices of r.m.s. amplitude of the secondary perturbations for x/c positions of 0.289, 0.307, 0.325, 0.343, 0.361, 0.379 (see upwards), the contours step is 2 per cent of U_0, y^{**} is momentum thickness.

direction that, obviously, is connected to influence of the adverse pressure gradient. As a whole, the transverse spreading angle of disturbed area downstream in case of an adverse pressure gradient (see Figs. 4–6, and 8) is $\alpha = 34°$.

Now we shall consider the spatial pictures of secondary high-frequency disturbances evolution together with its influence on average flow characteristics ($u' + \Delta U$) represented in the form of the disturbance amplitude isosurfaces for 10, 6, 4, 2, 0.9 % of U_0 and 0.4 % of U_0 (Fig. 9) and the spatial pictures of secondary high-frequency disturbances evolution (u') shown in the form of the disturbance amplitude isosurfaces for 3 % of U_0, 2.7 % of U_0, 1.5 % of U_0, 0.9 % of U_0, 0.3 % of U_0, and 0.2 % of U_0 (Fig. 10). Such representation of isosurfaces for various amplitude levels allows us to see layer-

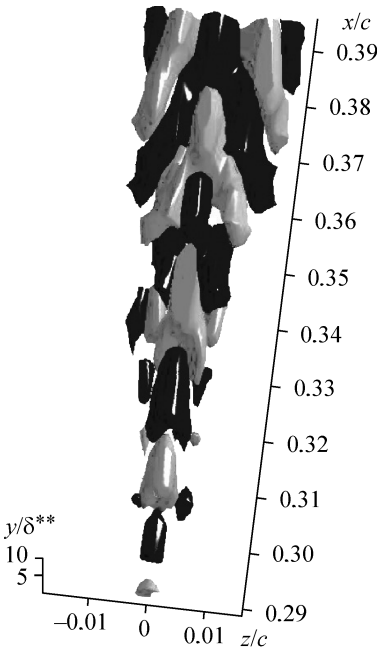

Fig. 6. 3D instantaneous distribution of the secondary disturbances (u') for the case $dp/dx > 0$. The minimum level of perturbations is 1.5 per cent of U_0.
The dark and light halftones indicate positive and negative velocity deviations.

wise and in detail internal structure of the disturbed flow area. For example, at a level of isosurfaces amplitude ($u' + \Delta U$) from 2 up to 10 % of U_0 in Fig. 9 it is possible to observe clearly streaky structure its streamwise modulation and transverse multiplication that it is practically impossible to find out at level of isosurfaces amplitude for ($u' + \Delta U$) = 0.4 % of U_0. A similar picture is observed in Fig. 10. At a level of isosurfaces amplitude (u') from 0.9 up to 3 % of U_0 the Λ-structures and their transverse multiplication are distinctly visible, that it is practically impossible to find out at a level of isosurfaces amplitude (u') for 0.2 and 0.3 % of U_0.

On the other hand, at a level of isosurfaces amplitude from 0.9 to 3 % of U_0 (see Fig. 10) the longitudinal vortices of streamwise modulation of the streaky structure can be observed at the initial stage of disturbances evolution that is typical of varicose instability of streaky structures. Further downstream process of Λ-vortices appearance and their transverse multiplication takes place.

Thus, detailed hot-wire measurements of a nonlinear stage of varicose instability development of the streaky structure generated by roughness element in the unswept wing boundary layer in region of an adverse pressure gradient have shown that secondary high-frequency breakdown of the streaky structure is related to Λ-structures origi-

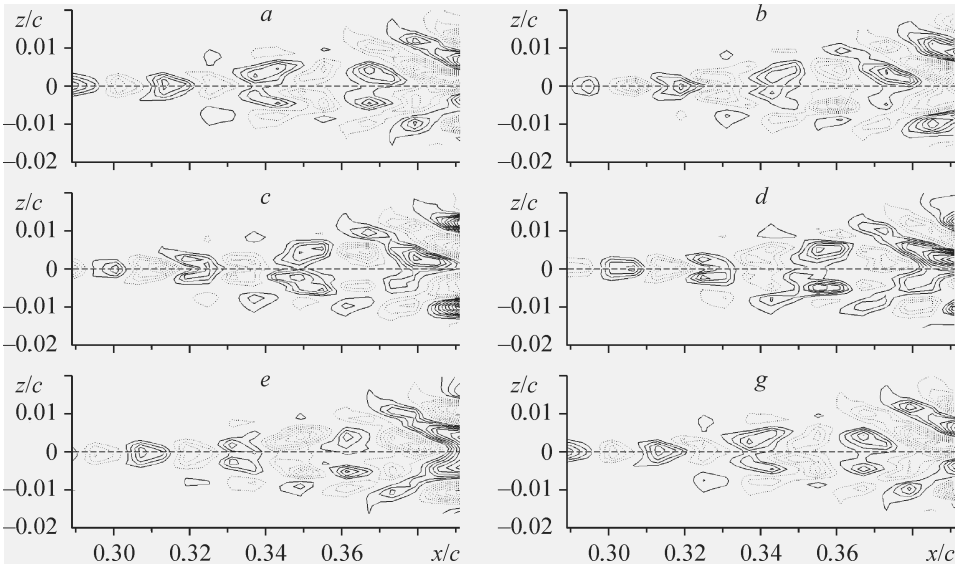

Fig. 7. Instantaneous distribution of the secondary disturbances in $x - z$ plane at y = 1.6 mm from the wall for the case $dp/dx > 0$, time sequence of pictures (*1-6*) from t = 0 ms (*1*) to t = 3 ms (*6*), Δt = 0.6 ms. Solid and dashed lines indicate positive and negative u'-deviations, the contours step is 1 per cent of U_0.

nation. The adverse pressure gradient favours the intensity growth both of the secondary high-frequency dist urbances and the streaky structure itself. This process results in an abrupt spatial spreading of the disturbed area due to the transverse multiplication of coherent structures. Finally, this leads to acceleration of the flow turbulisation.

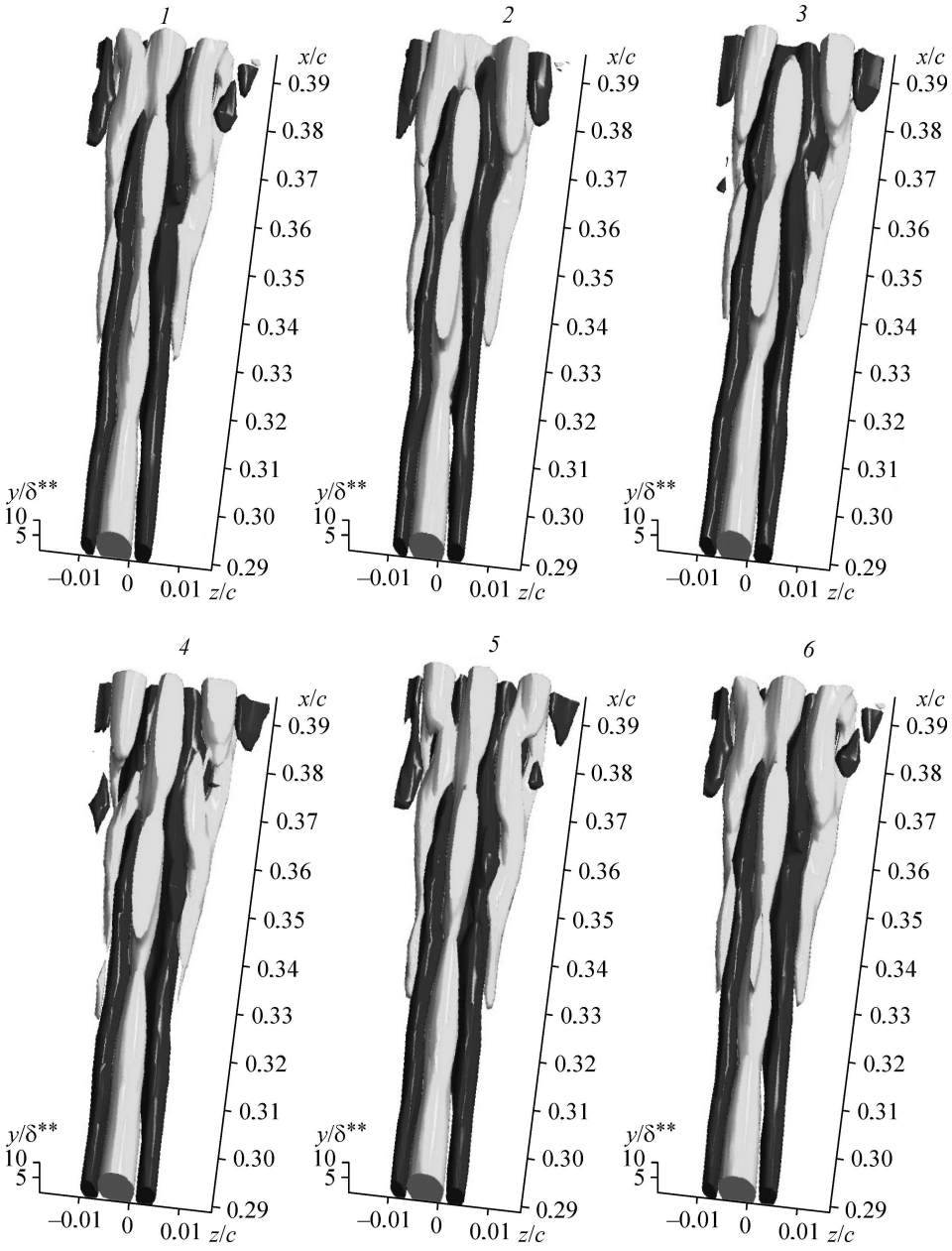

Fig. 8. 3D distribution of the instantaneous velocity deviation ($u' + \Delta U$) from the mean flow in undisturbed boundary layer for the case $dp/dx > 0$, time sequence of pictures (*1–6*) from $t = 0$ ms (*a*) to $t = 3$ ms (*g*), $\Delta t = 0.6$ ms. The minimum level of perturbations is 2.5 per cent of U_0, the dark and light halftones indicate positive and negative velocity deviations.

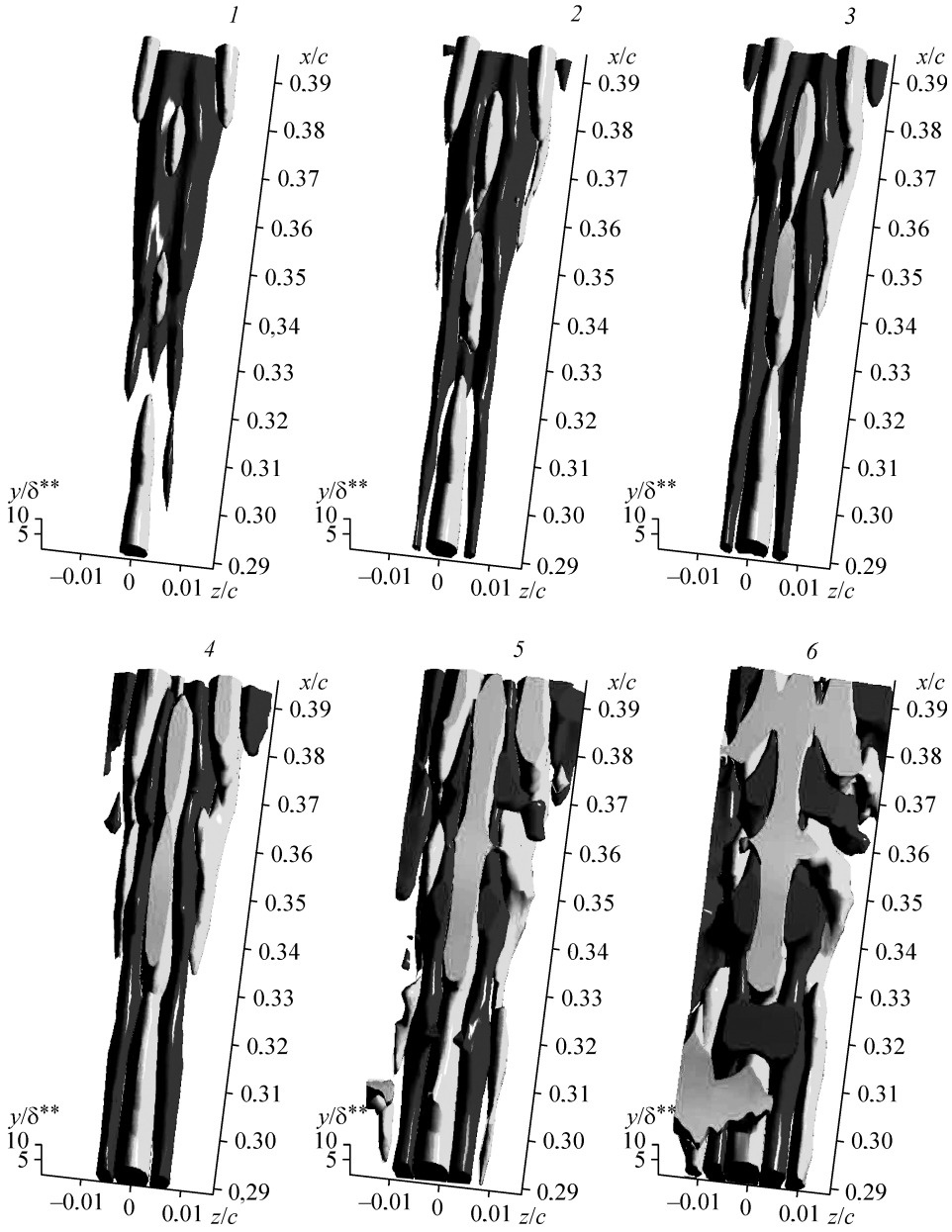

Fig. 9. 3D instantaneous distributions of the instantaneous velocity deviation ($u' + \Delta U$) from the mean flow in undisturbed boundary layer for the case $dp/dx > 0$ depending on amplitude of representing surface: 10 (*1*), 6 (*2*), 4 (*3*), 2 (*4*), 0.9 (*5*), and 0.4 % (*6*) of U. The dark and light halftones indicate positive and negative velocity deviations.

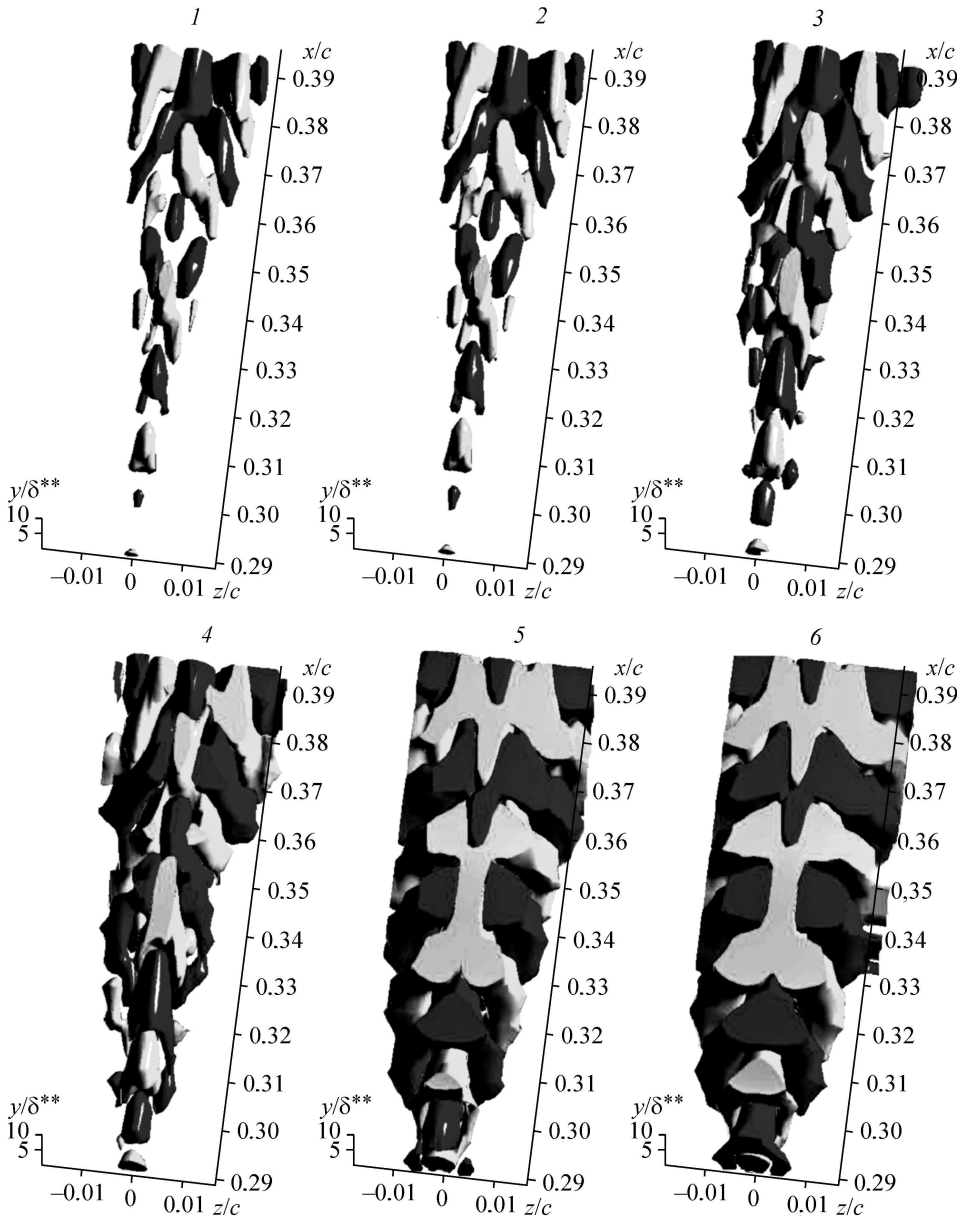

Fig. 10. 3D instantaneous distributions of the secondary disturbances for the case $dp/dx > 0$ depending on amplitude of representing surface: 3 (*1*), 2.7 (*2*), 1.5 (*3*), 0.9 (*4*), 0.3 (*5*), and 0.2 % (*6*) of U_0. The dark and light halftones indicate positive and negative velocity deviations.

4. DISCUSSION OF MEASUREMENT RESULTS AND CONCLUSIONS

Detailed spatio-temporal hot-wire measurements of varicose instability of the streaky structure generated by a roughness in an unswept wing boundary layer in region of the adverse pressure gradient have allowed to obtain the answers to the questions: what is the flow structure, what is the dynamics of coherent structures evolution, and what is the mechanism of flow turbulent breakdown at last stages of nonlinear varicose instability of the streak. It is known [30, 31] that the nonlinear stage of varicose instability of a flat plate flow at zero pressure gradient results in occurrence of the coherent structures such as Λ-vortices. Earlier [33], the experimental studies of varicose instability of a streaky structure generated by air blowing in the unswept wing boundary layer were carried out. Present studies were conducted under the same experimental conditions except the streaky structure excitation technique and the free stream velocity rate. In this case, the streaky structure is generated with the help of a roughness element, as well as in work [30]. However, as opposed to [30], the streaky structure varicose instability was studied in region of an adverse pressure gradient and at late stages of its nonlinear evolution as well as in work [33]. Due to the distinction in a way of the streaky structure generation in present case and in [33], where the intensity of stationary disturbance (streaky structure) was adjusted by air blowing rate, in our case it has been controlled by only change of free stream velocity. In this connection, the free stream velocity (U_0) was reduced from 8.3 m/s in [33] to 5.5 m/s because flow became turbulent at U_0 = 8.3 m/s. Comparison of changes of the mean velocity characteristics measured on the maximum velocity deviations $(U_{max} / U_{min})/2/U_0$ in region of an adverse pressure gradient downstream in the disturbed (xyz) space for the case of streaky structure excitation by air blowing [33] and by roughness is shown in Fig. 11. As can be seen, the intensity of mean velocity perturbation in initial area measurements (up to $(x - x_0) /c \approx 0.04$) reduces in both cases because of the disturbance transverse spreading. But further downstream, it begins to grow sharply reaching, approximately, 30 % of U_0 at $(x - x_0) / c = 0.1$ in case of the given experiment and more than 40 % of U_0 at $(x - x_0) / c = 0.09$ in [33]. In the latter case, it is possible to observe the intensity reduction of mean velocity perturbation at $(x - x_0) /c > 0.09$. In both cases, this process is especially nonlinear, though in the present experiments it is more weak than in work [33]. It is seen that along with transverse spreading of the disturbed area that has been shown above and in [33], there is a sharp growth of an adverse pressure gradient influence upon amplitude of the mean flow deformation especially in a situation of the streaky structure generation by air blowing [33].

As a whole, the graph shows that the nonlinear processes of secondary high-frequency breakdown of the streaky structures are related to their influence on the mean flow characteristics. It can be observed both from transverse redistribution of the disturbance energy and from total growth of one in case of an adverse pressure gradient. The secondary high-frequency disturbance behavior is the same, and space position of the flow breakdown into the turbulence state is related to evolution properties of the secondary high-frequency disturbance. Growth rates curves (r.m.s. fluctuations — u' measured in xyz space) of the secondary high-frequency disturbances downstream for both cases of streaky structures excita-

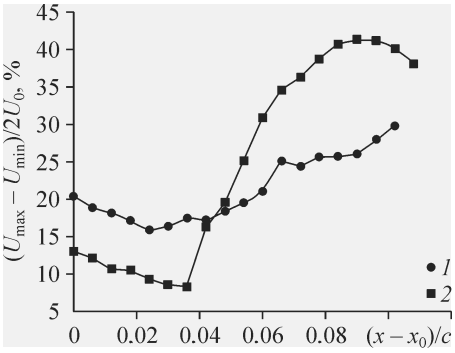

Fig. 11. Streamwise variations of the "peak to peak" magnitude of the mean flow distortion induced by the streaky structure excited by roughness (*1*) and air blowing (*2*, from [33]) at $dp/dx > 0$.

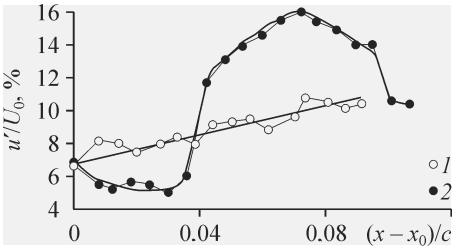

Fig. 12. Streamwise variations of the r.m.s. amplitude of the high-frequency secondary perturbations in case of streaky structure excited by roughness (*1*) and air blowing (*2*, from [33]) at $dp/dx > 0$.

tion are shown in Fig. 12. It is seen that in the initial area of measurements the disturbance amplitude reduces slightly (from 6–7 % of U_0 up to 4–5 % of U_0) in a range of $(x - x_0) / c \approx$ 0–0.04, however, further downstream, it grows reaching approximately 16 % of U_0 at $(x - x_0) / c = 0.07$ and then begins to reduce indicating on the flow turbulisation for a case from [33]. In a case of the present study, the disturbance amplitude increasing occurs much more slowly. It reaches magnitude about 10 % of U_0 at $(x - x_0) / c = 0.09$ and continues to grow further downstream, but transition to turbulence is not observed. Thus, it is necessary to draw a conclusion from Figs. 11 and 12 that the tendency of varicose instability growth of the streaky structures generated by various methods in unswept wing boundary layer in region of adverse pressure gradient was kept. However, if in the case from work [33] it is observed flow turbulisation, in the present case it should come much later in space, probably due to a weaker nonlinearity or features of development of the streaky structure generated by a roughness which intensity directly depends on free stream velocity that demands additional studies. Nevertheless, the spatio-temporal hot-wire visualization of a nonlinear stage of the streaky structures varicose instability in region of an adverse pressure gradient in unswept wing boundary layer shows the same disturbances evolution for both cases of the streaks excitation. It should be noted the following disturbances evolution features: the Λ-structures origination, multiplication of these coherent structures and streaky structures, transverse spreading of the disturbed area irrespective of the generation way of the initial streaky structures that it is possible to observe in Fig. 13. It shows, for comparison, the isosurfaces of the velocity fluctuations amplitudes (u') in (xyz) space for a case of streaky structure generation by air blowing at a zero and adverse pressure gradient (it is taken from [33]) and result of the present studies. One can see from Fig. 13 that the angle of the disturbed area transverse spreading is different for all three cases. In case of the disturbance evolution in area with a zero pressure gradient, it is approximately 23°, and in area of an adverse pressure gradient it equals 40°, that almost twice it is more (by results of studies from the work [33]). As it is seen from results of the present studies, the angle of the disturbed area transverse spreading is approximately 34° in case of an adverse pressure gradient, that, in comparison with a similar situation from work [33], is much less. It is connected probably, as it was already marked above, with a weaker nonlinear process in comparison with [33] due to the complexities with selection of the streaky structure intensity dependent on the free stream velocity.

As a whole, the detailed measurements allowed us to obtain the spatial-temporal pictures of flow and contour diagrams of its structure confirming a conclusion that the adverse pressure gradient for last stages of nonlinear evolution of the streaky structure varicose instability results in acceleration of the flow turbulisation in comparison with its development in region of a zero pressure gradient irrespective of a way of the streaky structures excitation. On the basis of these studies it is possible to make the following basic conclusions:

– it is found that the mechanism of the streaky structures nonlinear breakdown in the unswept wing boundary layer in region of an adverse pressure gradient is closely related to the process of their secondary high-frequency varicose instability accompanied by coherent structures appearance, such as Λ-vortices;

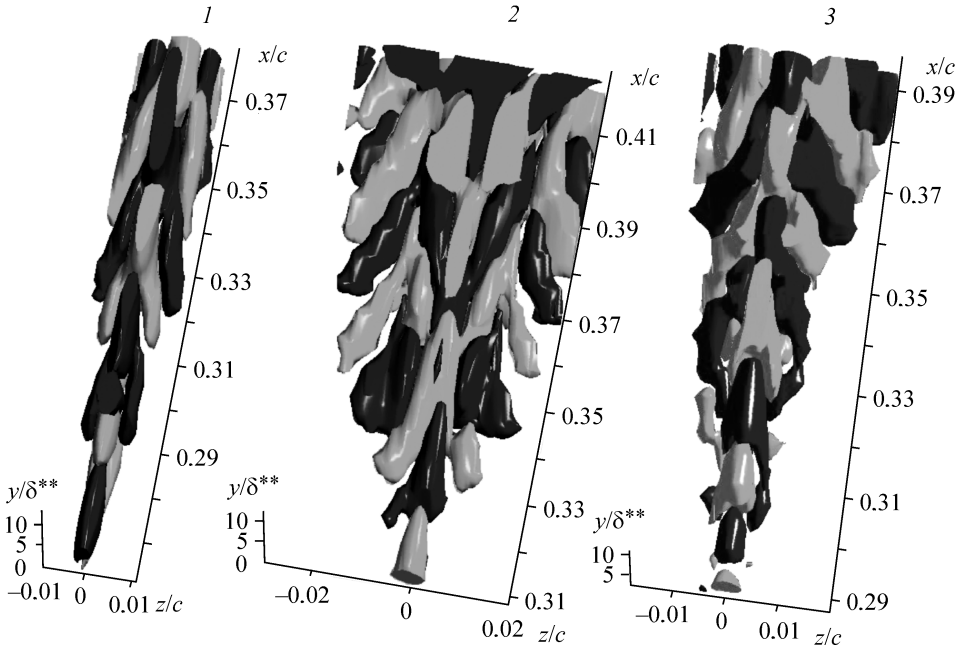

Fig. 13. Comparison of the 3D instantaneous distributions of the secondary disturbances (u') of the varicose instability of streaky structure excited by air blowing (*1* — $dp/dx = 0$, *2* — $dp/dx > 0$) and roughness (*3* — $dp/dx > 0$) in unswept wing boundary layer: *1,2* (from [33]), *3* (from this work). The minimum level of perturbations is 9.0 per cent of U_0, the dark and light halftones indicate positive and negative u'-deviations.

– it is shown that secondary high-frequency varicose instability of the streaky structure at a nonlinear stage of its evolution in the unswept wing boundary layer in region of an adverse pressure gradient results in multiplication of both the streaky structures and Λ-vortices downstream;

– it is found that the main flow structural characteristics of nonlinear varicose instability of the streaky structures in region of adverse pressure gradient in the unswept wing boundary layer do not depend on a way of the streaky structure excitation both by air jet blowing in a boundary layer and with the help of the local flow heterogeneity.

REFERENCES

1. **Y.S. Kachanov, V.V. Kozlov, and V.Ya. Levchenko,** Occurrence of turbulence in a boundary layer, Nauka, Novosibirsk, 1982.
2. **P.S. Klebanoff, K.D. Tidstrom, and L.M. Sargent,** The three-dimensional nature of boundary-layer instability, J. Fluid Mech., 1962, Vol. 12, Pt. 1, P. 1–34.
3. **W.S. Saric, V.V. Kozlov, and V.Ya. Levchenko,** Forced and unforced subharmonic resonance in boundary layer transition, AIAA Paper 84-0007, 1984.
4. **Y.S. Kachanov,** On a universal mechanism of turbulence production in wall shear flows, Notes on Numerical Fluid Mechanics and Multidisciplinary Design. Vol. 86, Recent Results in Laminar-Turbulent Transition, Springer-Verlag, Berlin et al., 2003, P. 1–12.
5. **A.V. Boiko, G.R. Grek, A.V. Dovgal, and V.V. Kozlov,** The Origin of Turbulence in Near-Wall Flows, Springer-Verlag, Berlin et al., 2002.
6. **R.L. Panton,** Overview of the self-sustaining mechanisms of wall turbulence, Progress in Aerospace Sci., 2001, No. 37, P. 341–383.
7. **J.M. Floryan,** On the Goertler instability of boundary layers, Ibid., 1991, Vol. 28, P. 235–271.
8. **H. Bippes,** Experimentelle Untersuchung des laminar-turbulenten Umschlags an einer parallel angestroemten konkaven Wand, in: Mathematischnaturwissenschaftliche Klasse, Heidelberger Akademie der Wissenschaften, Sitzungsberichte, 1972, No. 3, S. 103–180 (also NASA-TM-75243, March 1978).

9. **A. Ito,** Breakdown structure of longitudinal vortices along a concave wall, J. Japan Soc. Aerospace Sci., 1985, Vol. 33, P. 166–173.
10. **P.R. Pratt, V.G. Chernorai, A.A. Bakchinov, and L. Loefdahl,** A quantitative flow visualization of a point source disturbance in a swept wing boundary layer, in: Book of abstracts EUROMECH Colloquium 423 " Boundary Layer Transition in Aerodynamics ", Stuttgart, 2001.
11. **M.S. Acarlar and C.R. Smith,** A study of hairpin vortices in a laminar boundary layer. Pt. 1, J. Fluid Mech., 1987, Vol. 175, P. 1–41.
12. **H.A. Haidary and CR. Smith,** The generation and regeneration of single hairpin vortices, J. Fluid Mech., 1994, Vol. 227, P. 127–135.
13. **G.R. Grek, V.V. Kozlov, M.M. Katasonov, and V.G. Chernorai,** Experimental study of a Λ-structure and its transformation into the turbulent spot, Current Sci., 2000, Vol. 79, No. 6, P. 781–789.
14. **U. Rist, K. Moeller, and S. Wagner,** Visualization of late-stage transitional structures in numerical data using vortex identification and feature extraction, in: Proc. 8th Int. Symp. Flow Visualization, Sorrento, Italy, 1998.
15. **J. Reuter and D. Rempfer,** A hybrid spectral/finite-difference scheme for the simulation of pipe-flow transition, Laminar-Turbulent Transition, H. Fasel and W.S. Saric (Eds.), Springer-Verlag, Berlin et al., 2000, P. 383–390.
16. **J. Zhou, R.J. Adrian, S. Balachandar, and T.M. Kendal,** Mechanisms for generating coherent packets of hairpin vortices in channel flow, J. Fluid Mech., 1999, Vol. 387, P. 353–396.
17. **R.J. Adrian, C.D. Meinhart, and C.D. Tomkins,** Vortex organization in the outer region of the turbulent boundary layer, J. Fluid Mech., 2000, Vol. 422, P. 1–23.
18. **V.V. Kozlov, G.R. Grek, L.L. Loefdahl, V.G. Chernorai, and M.V. Litvinenko,** Role of the longitudinal located structures during transition to turbulence in boundary layers and jets (Review), J. Appl. Mech. Tech. Phys., 2002, Vol. 43, No. 2, P. 62–76.
19. **M.V. Litvinenko, V.V. Kozlov, G.V. Kozlov, and G.R. Greek,** Influence of longitudinal streaky structures on process of tripping a round jet, J. Appl. Mech. Tech. Phys., 2004, Vol. 45, No. 3, P. 50–61.
20. **F. Li and M.R. Malik,** Fundamental and subharmonic secondary instabilities of Goertler vortices, J. Fluid Mech., 1995, Vol. 82, P. 255–290.
21. **A. Bottaro and B.G.B. Klingmann,** On the linear breakdown of Goertler vortices, Europ. J. Mech., B/Fluids., 1996, Vol. 15 (3), P. 301–330.
22. **M. Skote, J.H. Haritonidis, and D.S. Henningson,** Varicose instabilities in turbulent boundary layers, Phys. Fluids, 2002, Vol. 4, No. 7, P. 2309–2323.
23. **F. Waleffe,** On a self-sustaining process in shear flows, Phys. Fluids, 1997, Vol. 9, P. 883–896.
24. **G. Kawahara, J. Jimenez, M. Uhlmann, and A. Pinelli,** The instability of streaks in near-wall turbulence, Center for Turbulence Research, Annual Research Briefs, 1998, P. 155–170.
25. **W. Schoppa and F.Hussain,** Genesis and dynamics of coherent structures in near-wall turbulence: A new look, Computational Mechanics Publication, Southampton, UK and Boston, USA, 1997, P. 385–422.
26. **J. Jimenez and P. Moin,** The minimal flow unit in near-wall turbulence, J. Fluid Mech., 1991, Vol. 225, P. 213–226.
27. **J.H. Hamilton, J. Kim, and F. Waleffe,** Regeneration of near-wall turbulence structures, J. Fluid Mech., 1995, Vol. 287.
28. **L. Brandt and D.S. Heningson,** Transition of streamwise streaks in zero-pressure gradient boundary layers, J. Fluid Mech., 2002, Vol. 472, P. 229–261.
29. **S.K. Robinson,** The kinematics of turbulent boundary layer structure, NASA TM 103859, 1991.
30. **M. Asai, M. Minagawa, and M. Nishioka,** The stability and breakdown of near-wall low-speed streak, J. Fluid Mech., 2002, Vol. 455, P. 289–314.
31. **J.A. Litvinenko, V.G. Chernorai, V.V. Kozlov, L. Loefdahl, G.R. Greek, and H. Chun,** Nonlinear sinusoidal and varicose instability in the boundary layer (Review), Thermophysics and Aeromechanics, 2004, Vol. 11, No. 3, P. 329–353.
32. **J.A. Litvinenko, G.R. Grek, V.V. Kozlov, L. Loefdahl, and V.G. Chernorai,** Experimental investigation streaky structures varicose instability in a swept wing boundary layer of a sliding wing, Thermophysics and Aeromechanics, 2004, Vol. 11, No. 1, P. 13–21.
33. **Yu. A. Litvinenko, V.G. Chernorai, V.V. Kozlov, G.R. Grek, L.L. Loefdahl, and H.H. Chun,** Adverse pressure gradient effect on nonlinear varicose instability of a streaky structure in unswept wing boundary layer, Phys. Fluids, 2005, Vol. 17, No. 1, P. 118106 (1)–118106 (3).
34. **P. Corbett and A. Bottaro.** Optimal perturbations for boundary layers subject to stream-wise pressure gradient, Phys. Fluids, 2000, Vol. 12, No. 1, P. 120–130.